



Technical Note

# Water Levels in the Major Reservoirs of the Nile River Basin—A Comparison of SENTINEL with Satellite Altimetry Data

Prakrut Kansara \* and Venkataraman Lakshmi

Engineering Systems and Environment, University of Virginia, Charlottesville, VA 22904, USA

\* Correspondence: phk5e@virginia.edu

**Abstract:** With the increasing number of reservoirs on the Nile River Basin, it has become important to understand the reservoir operations in the basin for coordinated water management among the various countries. With the lack of a proper framework for data sharing amongst the Nile basin countries, satellite remote sensing provides a simple transparent way to continuously monitor the changes taking place in reservoirs in all regions of the Nile River Basin. This paper presents a comparison between Sentinel-1- and Sentinel-2-derived reservoir water levels and the altimetry-based water level from G-REALM (Global Reservoirs and Lakes Monitor) for three major reservoirs downstream of the Millennium Reservoir impounded by the Grand Ethiopian Renaissance Dam (GERD) on the Nile River for the period of 2014–2021. Water surface extents were derived from Sentinel-1 using dynamic thresholds and from Sentinel-2 with the use of the NDWI (Normalized Difference Water Index). The water levels were estimated using a DEM-based contour matching technique. For Roseires Reservoir, the water levels from Sentinel agreed well with those from G-REALM (RMSE = 0.92 m;  $R^2 = 0.82$ ). For Lake Nasser, the water levels also agreed well (RMSE = 0.72 m;  $R^2 = 0.85$ ). For Lake Merowe, there was a significant mismatch in the derived water levels, mostly due to a lack of sufficient data from both sources. Overall, satellite imagery from Sentinel provides a very good alternative to altimetry-based water levels for the Nile River Basin.

**Keywords:** Hydrology; Nile watershed; Sentinel-1; Sentinel-2; satellite altimetry; Nile reservoirs



**Citation:** Kansara, P.; Lakshmi, V. Water Levels in the Major Reservoirs of the Nile River Basin—A Comparison of SENTINEL with Satellite Altimetry Data. *Remote Sens.* **2022**, *14*, 4667. <https://doi.org/10.3390/rs14184667>

Academic Editor: Guy J.-P. Schumann

Received: 18 August 2022  
Accepted: 14 September 2022  
Published: 19 September 2022

**Publisher's Note:** MDPI stays neutral with regard to jurisdictional claims in published maps and institutional affiliations.



**Copyright:** © 2022 by the authors. Licensee MDPI, Basel, Switzerland. This article is an open access article distributed under the terms and conditions of the Creative Commons Attribution (CC BY) license (<https://creativecommons.org/licenses/by/4.0/>).

## 1. Introduction

Water resources management plays an important role in the understanding and assessment of available water to support domestic and economic activities globally. Access to hydrological data is critical for effective water resources management. In transboundary watersheds, the accessibility of hydrological data among the countries sharing the water resources is a major concern. There are multiple reasons contributing to this problem, including a lack of observations, observations of poor quality, and the lack of data sharing policies. Effective transboundary resource management requires a holistic understanding of river discharge, reservoir storage, and water use for the countries in the river basin to meet regional water demand. Transboundary river basins like the Nile, Indus, and Mekong currently suffer from high water stress due to increased water usage to support a constantly growing population and reduced streamflow from the presence of dams in upstream areas of the catchments. The dams on these rivers support hydropower generation and increased water storage for resilience towards the changing climate [1]. The management of water resources in these basins is subjected to challenges related to data sharing and lack of in situ observations [2]. There has been a constant decline in the network of in situ observation sites throughout the world, but especially in developing countries, which further exacerbates this problem of water resources management [3].

The Nile River Basin faces water resources management challenges due to a lack of publicly available data. The Nile River Basin covers 3.3 million km<sup>2</sup> and 11 countries (Figure 1). The Nile is approximately 6650 km long and traverses through varying climates,

including equatorial lakes, savannah, the Sahara Desert, and, ultimately, the Mediterranean climate at its outlet. One of the major challenges for water resources management in the Nile is the presence of large dams, especially in the downstream part of the river. High Aswan Dam (HAD), which is the largest embankment dam in the world, impounds Lake Nasser. Lake Nasser can hold up to 132 billion cubic meters of water, which is enough to sustain Egypt's water demand for at least two years [4]. Large dams regulate the flow of water at downstream end, which can create management problems in regions where there is a lack of data sharing policy in terms of flow regulation and water storage. With the start of Millennium Reservoir filling behind the Grand Ethiopian Renaissance Dam (GERD) in Ethiopia in July 2020, the seasonal flows in the Nile River are expected to be regulated even more, which will create additional management challenges. The presence of these dams changes the water regime and availability not only locally, but at the basin scale. The Nile Basin Initiative (NBI) was started in order to promote and manage equitable usage of the water resources of the Nile [5]. The NBI has identified a need for basin-wide access to river flow and reservoir operation data.

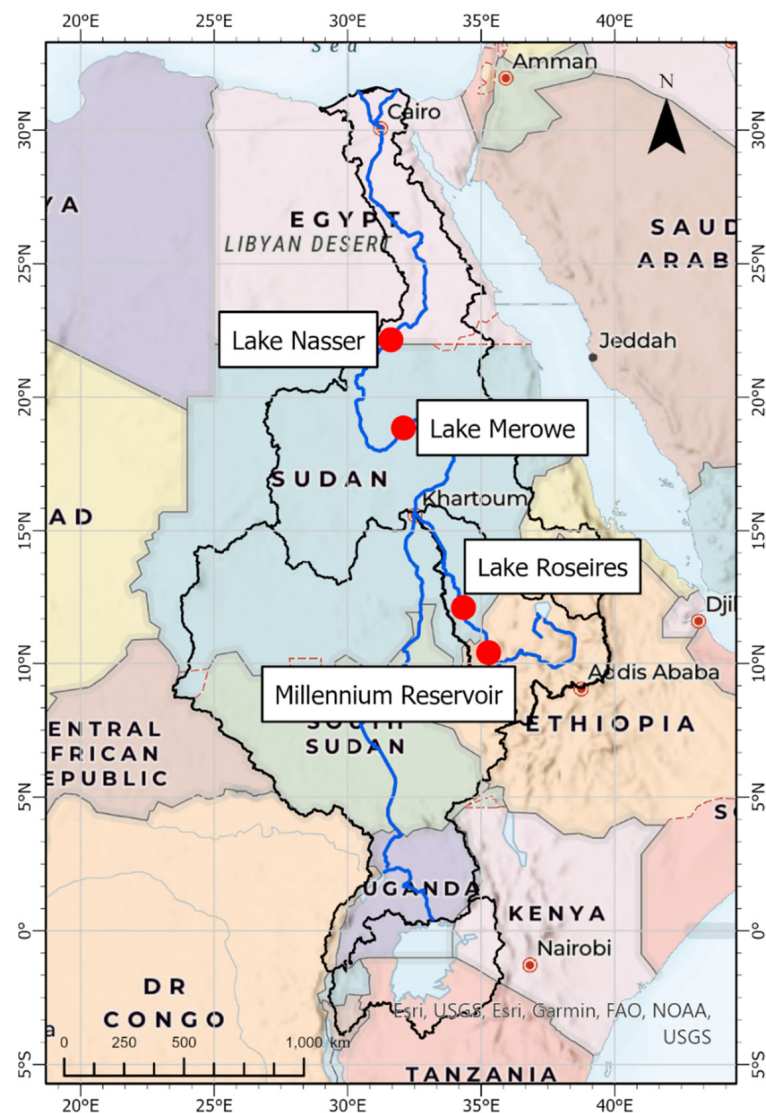


**Figure 1.** The Nile River basin and the reservoirs on the main channel of the Nile and the Blue Nile Rivers. The shapefiles for watershed boundaries and the river network were downloaded from the World Bank Data Catalog (<https://datacatalog.worldbank.org/search/dataset/0042032>, accessed on 12 April 2022).

Remote sensing observation is emerging as a technique to support hydrological monitoring and inform water resources management globally. Advancements in the processing of satellite data have increased the feasibility of monitoring water resources from space. Multispectral satellite missions like Sentinel, Landsat, and satellite altimetry missions like TOPEX/POSEIDON have been successfully used to derive water level data in lakes, reservoirs, rivers, floodplains, and wetlands, providing data for more than 15 years [6–10]. These satellite data products have wide applications in reliable estimation of water surface extents for inland water bodies and water levels [11,12]. The water level data derived from satellite altimetry have been combined with in situ measurements to estimate water storage in lakes and reservoirs, with successful applications in different parts of the world [13]. Duan and Bastiaanssen [14] proposed a method using only satellite altimetry and imagery data to estimate the volume variations of Lake Tana (Ethiopia) and Lake Mead (USA), and Kansara et al. [15] proposed a Sentinel-based contour matching approach to estimate the volume variations to track the Millennium Reservoir filling process.

Altimetry data are a direct measurement of the water level heights for inland water bodies like reservoirs, but they have a few limitations. The orbital path of the satellite altimeters does not always align with the deepest cross section of the lake [16–18]. Dettmering et al. [19] identified the limitations of satellite altimetry and concluded that the current altimeter configuration misses at least 9% of the global reservoirs greater than 100 km<sup>2</sup>, through a case study of the Mississippi River Basin. In addition, for the smaller lakes which are of size less than 100 km<sup>2</sup>, the satellite altimeter orbital track would only cover a small length of the lake, which could lead to inaccurate depth information for the reservoir. Another approach to water level estimation is the use of DEM contour matching of the surface water extents derived from Sentinel-2/3 or Landsat optical data. However, the optical data from these satellites have a limitation in terms of temporal coverage due to the presence of clouds, especially during the wet season [20,21]. On the other hand, Sentinel-1 is not affected by the presence of clouds due to the C-band Synthetic Aperture Radar (SAR) which can penetrate through the clouds and provide observations that are of great significance during the wet/flooding season when reservoir water levels are changing rapidly [22,23]. In addition, with the Surface Water and Ocean Topography (SWOT) mission focused on improved altimetry set to start collecting data in late 2022 [24], the need for Sentinel-derived surface water levels will be reduced. However, the data from SWOT have not been validated globally, and a comparison for SWOT-derived water levels is needed to validate all the different approaches used in this study.

The motivation for this study is to provide a comparison of the reservoir surface water extent and water level estimation process using Sentinel-1 and Sentinel-2 satellite imagery and satellite altimetry data. This study will provide a basis for future management decisions for the operation of the Millennium Reservoir and its potential impacts on reservoir operations in the downstream countries—Egypt, Sudan, and Ethiopia. To promote public usability of this research, we used the open-source coding language (Python) to analyze the SAR images, as well as for analyzing the results, and the codes will be publicly available through GitHub ([https://github.com/prakrutkansara/data\\_share/tree/main/rs\\_nile\\_reservoirs\\_2022](https://github.com/prakrutkansara/data_share/tree/main/rs_nile_reservoirs_2022), accessed on 15 August 2022).

## 2. Methods

### 2.1. Study Areas

#### 2.1.1. Lake Nasser

Lake Nasser is the reservoir formed by the impoundment behind the HAD, after the dam was built in 1971 in Egypt. Lake Nasser is one of the largest man-made lakes in the world and serves as the water bank for Egypt. A part of Lake Nasser falls within the Sudanese geographical boundaries, where it is called Lake Nubia. For the purpose of this study, the authors refer to Lake Nasser and Lake Nubia combined as Lake Nasser in general. The entire reservoir is approximately 500 km in length, out of which 330 km lies in Egypt and 170 km lies in Sudan (Figure 1). Lake Nasser is surrounded by desert,

with Arabian desert to its east and sand dunes and depressions to the west. The reservoir spans a maximum surface area of approximately 5250 km<sup>2</sup> after the peak flooding season in mid-October. Due to the large surface area of the reservoir, there is a significant amount of evapotranspiration over the reservoir. With the drier climate, the evapotranspiration rates are as high as 2400 mm/yr [25]. Water from the Nile River flowing into the reservoir is the only source of water for the reservoir. Rainfall over the reservoir is sparse, with an annual average amount of 15 mm (Figure 2a). The water levels in the reservoir are maintained at 175 m Above Mean Sea Level (AMSL) at the beginning of the hydrologic year (1 August). When the water level reaches 180 m, the excess water is directed to the Toshka Depression and the emergency spillways on the western bank [26]. The maximum retention of 180 m is maintained until the end of November, and subsequently, the water is released from the reservoir for the rest of the hydrologic year until July.

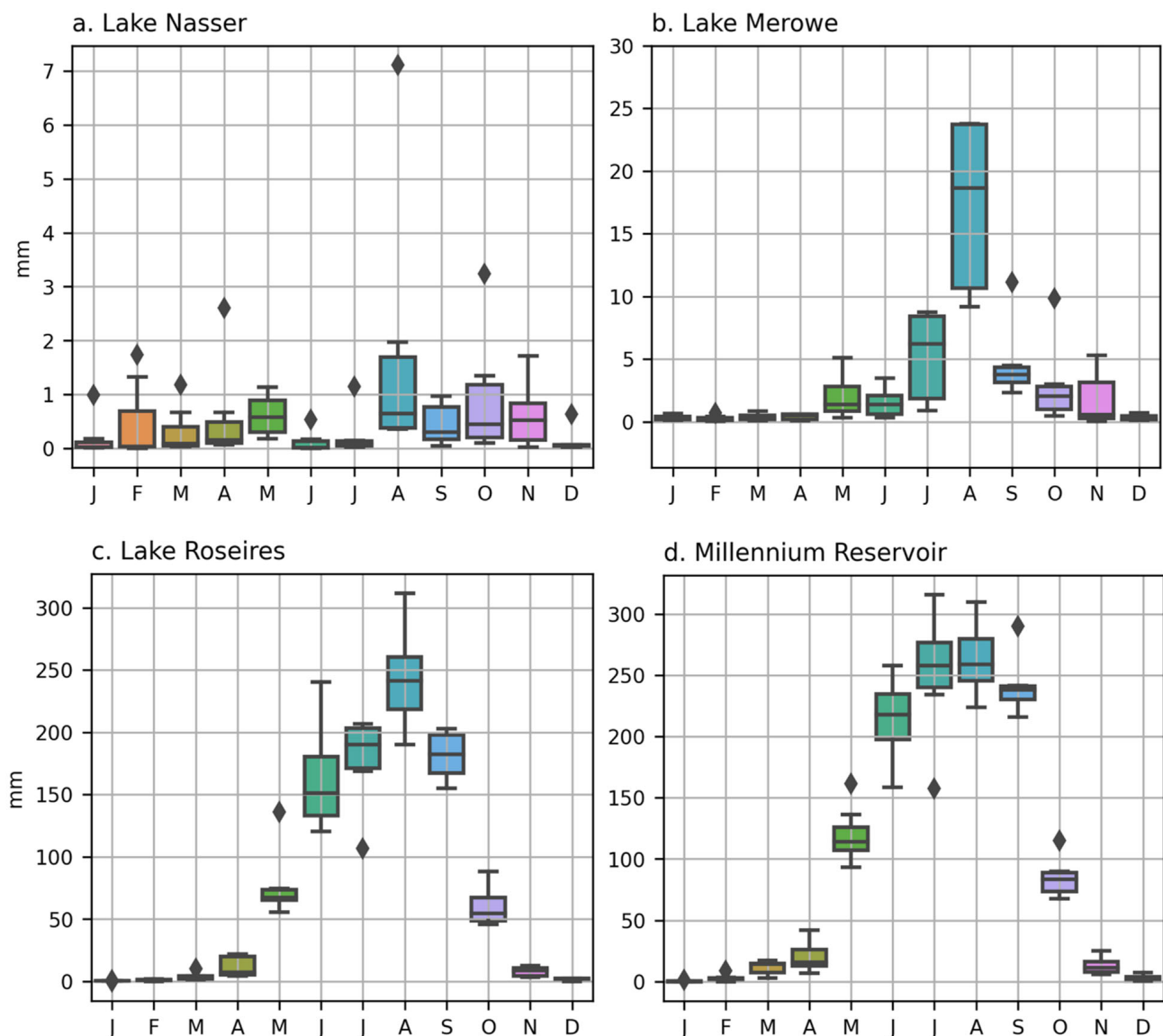


**Figure 2.** (a–d): Monthly boxplots of rainfall variation over the four reservoirs. The rainfall data were obtained from the GPM IMERG V6 Final Run product over the bounding box region of each reservoir. The diamonds represent the outliers beyond 95th percentile of the data.

### 2.1.2. Merowe Reservoir

Merowe Reservoir is a large reservoir on the Nile River in North Sudan (Figure 1). The reservoir was formed by the Merowe Dam, which became one of the largest hydroelectric

power projects in the African continent. Since the dam operation started in 2009, the Merowe Reservoir has expanded to cover approximately 476 km<sup>2</sup> surface area, and it can now hold up to 12.5 billion cubic meters of water, which is approximately 15% of the annual flow in the Nile. The main purpose of the construction of the Merowe Dam was to provide electricity to large urban centers of Northern Sudan, whereas other advantages like flood protection, sediment reduction, and the development of centralized agricultural schemes were also a part of the motivation for the construction of this dam [27]. Being surrounded by desert on all sides, the climate in this region is hot, dry, and arid. In addition, it receives less than 30 mm of annual rainfall (Figure 2b). Similar to Lake Nasser, water from the Nile River is the only major source of water for the Merowe Reservoir. The intended maximum water level is 300 m AMSL, whereas the minimum operating water level is approximately 285 m AMSL [28].

### 2.1.3. Roseires Reservoir

Roseires Reservoir is located on the Blue Nile in South-Eastern Sudan, approximately 100 km west of the Sudan–Ethiopia border (Figure 1). The topography surrounding the reservoir consists of steppes and lowlands with steep slopes bringing a significant amount of sediment. The dam was originally constructed in 1966, but due to major sedimentation issues reducing the dam storage capacity by approximately 30%, the dam was heightened by 10 m in 2013 [29]. The climate in the region is semi-arid, with much vegetation in the surrounding region. The dam was mainly constructed to improve access to irrigation and hydropower generation. The region receives 700 mm of annual rainfall, but water from the Nile River still remains a significant source of water for the reservoir (Figure 2c). The reservoir spans a surface area of approximately 290 km<sup>2</sup> and has a maximum storage capacity of 7.5 billion cubic meters. The minimum operating water level is 470 m AMSL, whereas the maximum water level capacity is at 480 m AMSL.

### 2.1.4. Millennium Reservoir

The Millennium Reservoir was formed as a result of the construction of the GERD in July 2020 near the Ethiopian–Sudanese border. The reservoir is built on the Blue Nile River, located approximately 15 km east of the Ethiopia–Sudan border inside Ethiopia (Figure 1). The region receives, on average, 1100 mm of annual rainfall (Figure 2d). The major source of water is the runoff merging into the Blue Nile River, starting from Lake Tana in the Ethiopian highlands. The surface area of the Millennium Reservoir is planned to be approximately 1875 km<sup>2</sup>. The GERD will provide 6.45 GW of hydroelectric power to Ethiopia at its full capacity and store 74 billion cubic meters of water. The reservoir filling process completed its second phase in 2021, and the third phase is set to start in August 2022.

## 2.2. Data

### 2.2.1. Global Precipitation Mission (GPM)

The GPM provides global observations of rainfall and snow using a network of satellites launched by NASA, JAXA, CNES, ISRO, NOAA, and EUMETSAT [30]. GPM data are extensively used worldwide for forecasting of floods, droughts, and extreme precipitation and snow events. The data collected by this satellite are calibrated with data from other microwave and infrared satellite sources to create an improved and high-quality precipitation product. In this study, the Integrated Multi-satellitE Retrievals for GPM (IMERG) Final Run version 6 product was used at a spatial resolution of 0.1° for analysis for the period 2014–2021.

### 2.2.2. SENTINEL

In this study, we used a combination of Synthetic Aperture Radar (SAR) Sentinel-1 and optical Sentinel-2 imagery [31]. The main motivation behind using the two Sentinel products is because Sentinel-2 suffers from major cloud cover contamination during the wet

season. This does not allow for the usage of Sentinel-2 imageries for water mask creation. In order to overcome the unavailability of Sentinel-2 data, we leveraged the capabilities of Sentinel-1 SAR data, which can sense through the clouds. Since the threshold values to identify water from backscatter coefficients in a SAR image are empirical, we decide to compare both the Sentinel-1 and Sentinel-2 data with altimetry [31]. The Sentinel-1 SAR is a polar-orbiting twin satellite setup with a complementary ascending and descending pass over the Earth (Sentinel-1A and Sentinel-1B). It has a temporal repeat frequency of 6–12 days based on the geographical location of the area. Similar to Sentinel-1, Sentinel-2 also has a twin satellite setup with a 5-day temporal frequency at the equator. The optical sensor onboard Sentinel-2 has a 13-band multispectral imaging instrument (MSI) which senses data at spatial resolutions of 10 m, 20 m, and 60 m. The Sentinel data were downloaded from the European Space Agency (ESA) using the open hub cloud service.

### 2.2.3. SRTM

Elevation data were obtained from the Shuttle Radar Topography Mission (SRTM), which was launched in February 2000 to acquire complete near-global high-resolution data of Earth's elevation [32]. It is a global dataset providing gridded elevation values for the region between 60°N and 60°S at a spatial resolution of 30 m. The interferometric images at nadir are processed to obtain the elevation difference at a location on the Earth's surface. These images are then transformed into the Digital Elevation Model (DEM). We used the SRTM void filled 1/3 arc-second DEM data for our study.

### 2.2.4. G-REALM

The Global Reservoir and Lakes Monitor data (G-REALM) is a collection of altimetry data from multiple sources managed by the United States Department of Agriculture (USDA) [33]. The database manages the data from Topex/Poseidon, Jason-1, Jason-2, and Envisat. The altimetry water levels are provided at time intervals of 10 days for a majority of the lakes all across the world. G-REALM provides relative water levels with respect to the mean 9-year Topex/Poseidon water level.

## 2.3. Methods

### a. Delineation of Reservoir Surface Area:

The extents (surface areas) of the reservoirs were delineated from Sentinel satellite images (Figure 3) corresponding to the dates 20–31 October, 2021, representing the post-peak flooding season in the Nile River, using the Normalized Difference Water Index (NDWI) [34] as given by Equation (1):

$$\text{NDWI} = \frac{\text{GREEN} - \text{NIR}}{\text{GREEN} + \text{NIR}} \quad (1)$$

where *GREEN* and *NIR* are the green and near-infrared red bands, respectively. NDWI values range from −1 to 1, with water features having values between 0.2 and 1. The NDWI leverages the sharp contrast of water features in the green and near-infrared bands. Water features have high reflectance in the green band and low reflectance in the near-infrared band. A value of 0.5 or higher clearly represents water bodies, but values between 0.2 and 0.5 need to be identified via manual visual inspection. Values between 0 and 0.2 represent wet vegetation and soil moisture, and values below 0 represent other land features.

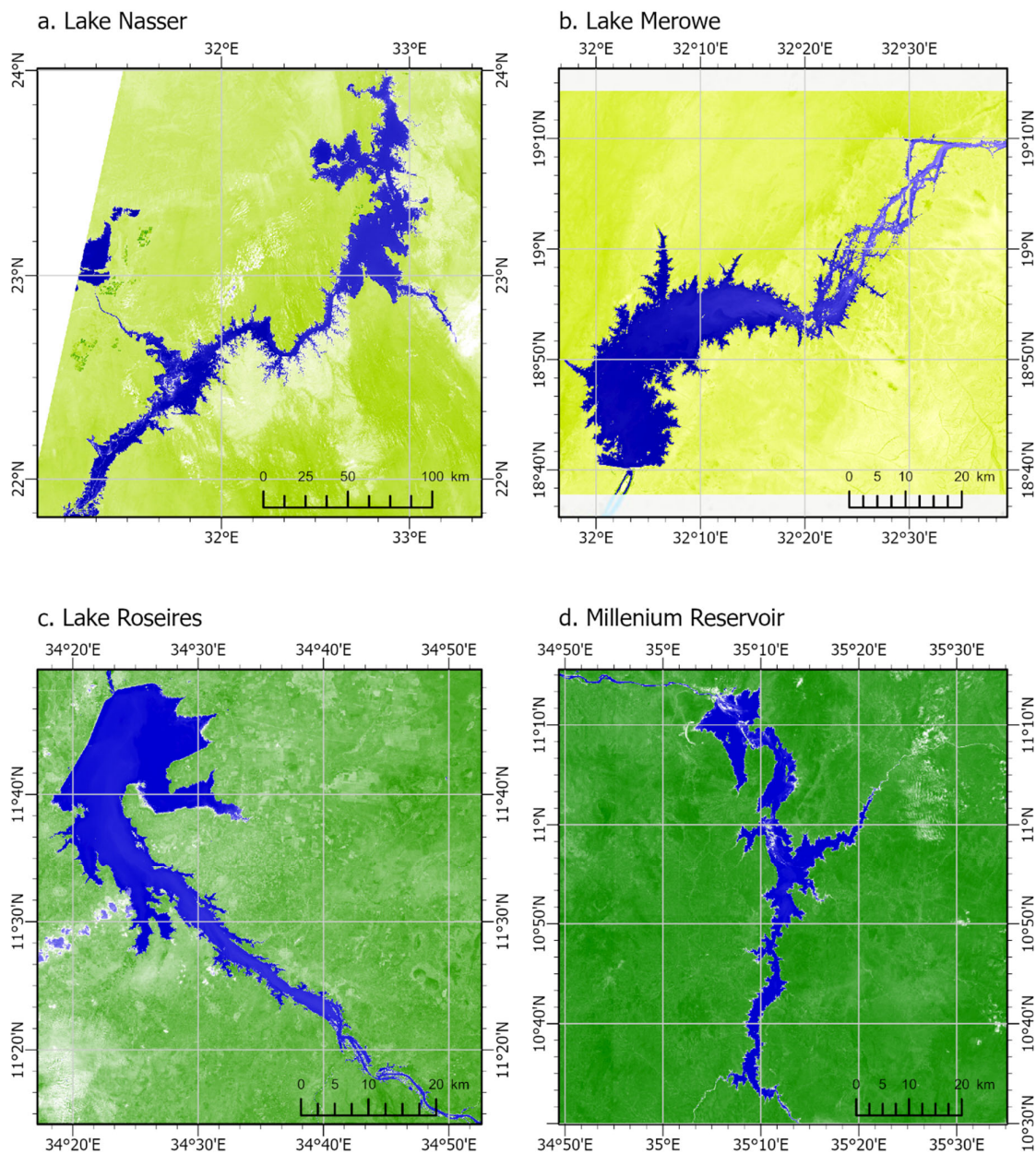


**Figure 3.** Surface water extent extracted using the water mask created from the NDWI using cloud-free Sentinel-2 images. The images show the surface water extent of four reservoirs in the Nile Basin, (a) Lake Nasser, (b) Lake Merowe, (c) Lake Roseires, and (d) Millennium Reservoir, after the peak flooding season corresponding to late October. These images correspond to the dates 20–31 October 2021, representing post-peak flooding surface water extents in the different reservoirs.

#### b. SAR image processing:

In this study, for Sentinel-1 SAR data, we used the GRD (Ground Range Detected) imagery in IW mode at 10 m spatial resolution. There are seven pre-processing steps involved before we can use the images to prepare a water mask. Each Sentinel-1 image was preprocessed using the following steps: (1) orbit file application, (2) thermal noise removal, (3) border noise removal, (4) calibration, (5) speckle filtering, (6) range Doppler terrain correction, and (7) conversion to dB values [35]. After preprocessing and converting the backscatter coefficients to dB for all images, a dynamic threshold of  $-15$  dB to  $-20$  dB (integer values) was used to prepare six different water masks from Sentinel-1 for each image. In addition, Sentinel-2 Level-2A main output data were used. These Sentinel-2 data

are orthorectified images that provide the Bottom-Of-Atmosphere (BOA) obtained after atmospheric correction of Level-1C products. These Sentinel-2 images were then classified using the Modified Normalized Difference Water Index (NDWI) calculated from the green and near-infrared (NIR) bands with 20 m spatial resolution to prepare the water masks for the dates where cloud cover was less than 30% of a single scene.

c. DEM-based water level estimation:

The water level was estimated using DEM-based contour matching with the surface water masks derived from Sentinel-1 and Sentinel-2. This approach was used to derive water levels in a Millennium Reservoir filling study by Kansara et al. [15]. We averaged out this per pixel calculation over the entire area where we detected water pixels using the Sentinel images.

### 3. Results

#### 3.1. Comparison of Sentinel-Derived Water Level with Altimetry-Based Water Level Estimates

##### 3.1.1. Lake Roseires

The time series of monthly water levels from Sentinel and G-REALM for Roseires Reservoir are shown in Figure 4 and Table 1. Figure 4 shows that water levels from Sentinel-1 G-REALM agreed well with the Sentinel water level measurements ( $R^2 = 0.82$ ) for high reservoir levels. However, water levels from G-REALM overestimated reservoir levels during the flood season. The flooding season begins in the month of June when the reservoir levels are at minimum and continues until the end of October, which leads to a maximum water level in the reservoir by the end/beginning of the calendar year (December/January). Because of the very high flow during the flood seasons of 2019 and 2020, the reservoir level rose above minimum levels. The RMSE of Sentinel-based water levels against G-REALM water levels for Roseires was 1.03 m, which is approximately 7.3% of the seasonal variation (~14 m), showing good agreement with in situ measurements. Several factors including water body size, topography of the surrounding region, and its roughness affect the accuracy of altimetry water levels. The variation of the RMSE ranges from 10 to 20 cm for large rivers, whereas for smaller rivers, the variation is within 3 cm. A higher variability in Sentinel data was observed during the drying phase of the reservoir (December–May). During the drying phase, as the water levels drop at the boundaries of the reservoir, there is more contamination and mixing of signals from the surrounding wet land.

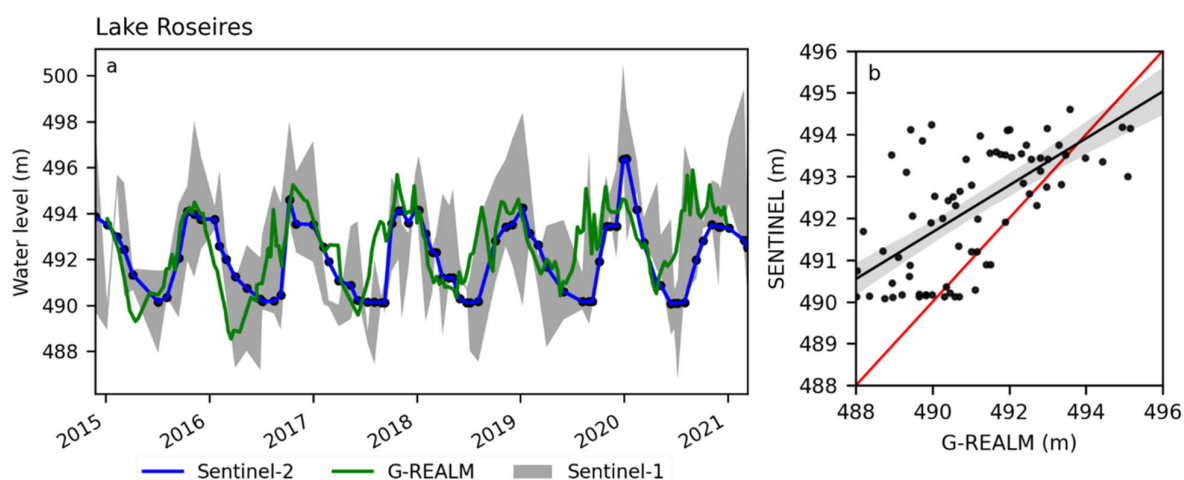


**Figure 4.** (a) Water levels estimated using contour matching from SRTM DEM with surface water extent derived from Sentinel-1, Sentinel-2, and G-REALM for Lake Roseires. The band of values for Sentinel-1 represents the water levels derived from threshold values ranging from  $-15$  to  $-20$  dB for extracting water masks. (b) Scatter plot showing the relationship between water levels estimated from Sentinel vs. G-REALM data.

**Table 1.** Average water levels derived from the two sources for Lake Roseires.

Reservoir Name	Year	Sentinel-1		Altimetry	
		No. of Images Available	Average Water Level (m)	No. of Data Points Available	Average Water Level (m)
Lake Roseires	2014	1	487	27	488
	2015	16	484	29	489
	2016	14	485	28	489
	2017	15	484	30	490
	2018	16	484	28	490
	2019	17	483	29	489
	2020	16	487	27	490
	2021	15	485	28	488

### 3.1.2. Lake Merowe

For Lake Merowe, Figure 5 and Table 2 show the water levels estimated using Sentinel, along with G-REALM altimetry data. From the Sentinel-derived water levels, the average water levels were in the range of 280–290 m for the time period of 2016–2021. The water levels did not show any increasing or decreasing trend over the years, with the highest and lowest water levels occurring in late 2020. There was only a limited number of data points available through altimetry. The altimetry data were present only for 2016–2019. The Sentinel-derived water levels were lower than the altimetry water levels for these years.

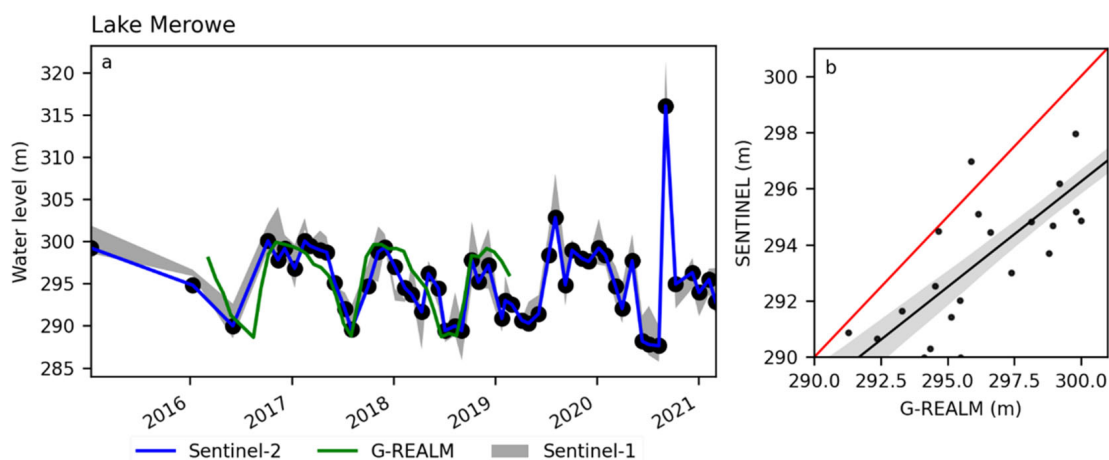


**Figure 5.** (a) Water levels estimated using contour matching from SRTM DEM with surface water extent derived from Sentinel-1, Sentinel-2, and G-REALM for Lake Merowe. The band of values for Sentinel-1 represents the water levels derived from threshold values ranging from  $-15$  to  $-20$  dB for the extraction of water masks. (b) Scatter plot showing the relationship between water levels estimated from Sentinel vs. G-REALM data.

The RMSE of Sentinel-based water levels against G-REALM water levels for Merowe was 2.4 m, which is about 24% of the seasonal variation ( $\sim 14$  m), and the  $R^2$  value was 0.76, showing average agreement with altimetry data. In addition, the bathymetry of Lake Merowe in the northern regions, which are seasonally flooded during the wet season, has significantly higher slope. This high slope leads to higher variations in the reservoir surface areas between consecutive months. For this reason, when a threshold is used to derive the surface water masks from Sentinel-1 backscatter signals, the possibility of signal contamination is significantly higher, leading to estimates with higher variability.

This effect is more intense for reservoirs that undergo larger seasonal variations, like Lake Merowe, leading to higher mismatch between the estimates.

**Table 2.** Average water levels derived from the two sources for Lake Merowe.

Reservoir Name	Year	Sentinel-1		Altimetry	
		No. of Images Available	Average Water Level (m)	No. of Data Points Available	Average Water Level (m)
Lake Merowe	2014	-	-	-	-
	2015	1	285	-	-
	2016	5	284	11	291
	2017	11	283	24	295
	2018	13	282	27	293
	2019	10	281	2	296
	2020	8	282	-	-
	2021	2	284	1	293

### 3.1.3. Lake Nasser

Figure 6 and Table 3 show the time series of Sentinel-derived and G-REALM altimetry-based water level variations. In Figure 6, both Sentinel-derived and altimetry water levels are in good agreement in their seasonal variations and magnitude, especially at high reservoir levels. The reservoir water levels showed a consistent decline from 2015 until the end of 2016, subsequently followed by a gradual increase in the water levels until the start of 2021. The RMSE of Sentinel-derived water levels against G-REALM water levels was 0.72 m, which is about 6% of the annual fluctuation (~13 m), while the  $R^2$  value was 0.85. The accuracy of Sentinel-1-derived water levels for Lake Nasser was lower as compared to that for Lake Roseires, partly due to its long and narrow shape, which contaminates altimetry products with the presence of land around it. This can be removed via manual processing of altimetry data, which is beyond the scope of this study. Details on the removal of land contaminations have been discussed by the developers of G-REALM.

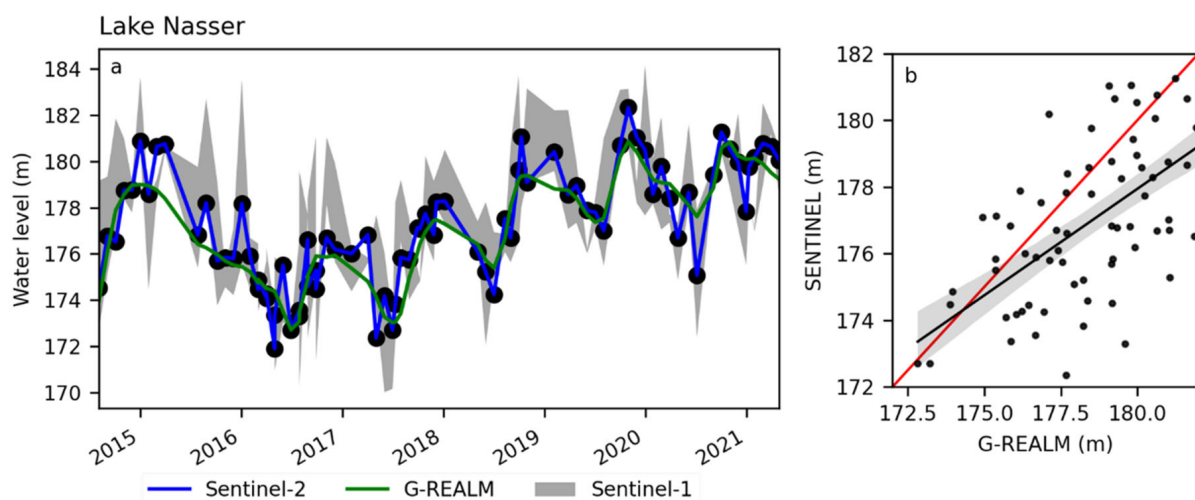


**Figure 6.** (a) Water levels estimated using contour matching from SRTM DEM with surface water extent derived from Sentinel-1, Sentinel-2, and G-REALM for Lake Nasser. The band of values for Sentinel-1 represents the water levels derived from threshold values ranging from  $-15$  to  $-20$  dB for the extraction of water masks. (b) Scatter plot showing the relationship between water levels estimated from Sentinel vs. G-REALM data.

**Table 3.** Average water levels derived from the two sources for Lake Nasser.

Reservoir Name	Year	Sentinel-1		Altimetry	
		No. of Images Available	Average Water Level (m)	No. of Data Points Available	Average Water Level (m)
Lake Nasser	2014	5	177	28	178
	2015	14	176	27	176
	2016	16	174	29	175
	2017	15	173	30	174
	2018	17	175	28	175
	2019	16	178	27	178
	2020	16	179	28	180
	2021	16	179	30	181

#### 4. Discussion

The Sentinel-derived water levels using Sentinel-1 and Sentinel-2 showed a reasonable match with the altimetry data from G-REALM. To derive the water masks from Sentinel-1 SAR data, in this study we used an empirical range of thresholds to account for the variability in capturing the seasonal changes in backscatter coefficients. Hence, the water level outputs in this study are stochastic. An ensemble mean of such probabilistic output would provide better information about the water levels when Sentinel-2 data are unavailable, due to presence of cloud cover. The water levels derived for Lake Roseires and Lake Nasser provide a better match as compared to those for Lake Merowe when validated with the altimetry data. The Sentinel data over Lake Merowe were sparsely available, and the altimetry data points were also very limited to validate the Sentinel-derived water level.

A comparison of the water levels in the four reservoirs (Lake Nasser, Lake Merowe, Lake Roseires, and Millennium Reservoir) is given in Figure 7 for 2015–2021 since there was inconsistent availability of data across all reservoirs. There was a significant change in the water levels in Lake Merowe and Millennium Reservoir in 2020, due to heavy flooding in the region. Lake Roseires and Lake Nasser did not reveal any such increase in water levels during this period. The reservoir operations did not show any abrupt changes, but they followed regular seasonal variations over the 6 years except for 2020, which is partly due to heavy flooding in Sudan. Such a comparison will help monitor the impacts on reservoir operations due to reservoir filling in the Millennium Reservoir. The mean height variation was 4 m for Lake Roseires, 7 m for Lake Merowe, 3 m for Lake Nasser, and 9 m for the Millennium Reservoir.

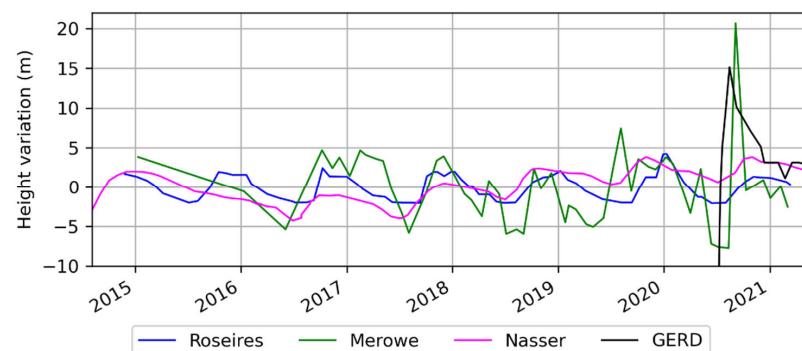


**Figure 7.** Comparison of height variations in all four reservoirs, including the Millennium Reservoir. The height variation was obtained by subtracting the mean water level height for each reservoir. The mean water level heights were 176 m for Lake Nasser, 294 m for Lake Merowe, 492 m for Lake Roseires, and 605 m for Millennium Reservoir.

Finally, the altimetry data also have limitations, including misalignment of the satellite track with the lake geography. The long and narrow lakes like Lake Nasser also suffer from contamination due to presence of land pixels in a single scene.

## 5. Conclusions

This study evaluated the feasibility and accuracy of water levels obtained using Sentinel-1 SAR data and Sentinel-2 optical data as compared with altimetry from G-REALM for three major reservoirs in the Nile River basin. First, the surface area was estimated from Sentinel-2 images using the NDWI and a range of thresholds for backscatter coefficients (−15 dB to −20 dB) from Sentinel-1. After the water surface area was derived from Sentinel data, the water level was estimated using DEM contour matching.

For Roseires Reservoir, water levels from Sentinel showed a good agreement with G-REALM (RMSE = 0.92 m,  $R^2 = 0.82$ ). Similarly, for Lake Nasser, water levels derived from Sentinel agreed well with G-REALM water levels (RMSE = 0.72 m,  $R^2 = 0.85$ ).

Based on the accuracy assessment and uncertainty analysis using dynamic thresholds, the results show the potential to use Sentinel data and leverage the combination of Sentinel-1 and Sentinel-2 to derive water levels where altimetry data are lacking, as in the case of Lake Merowe, which could be very useful for the context of monitoring reservoir operations. These estimated water levels not only provide critical insights on water releases to downstream users, but also give important information about the reservoir operation strategies.

This research contributes to bridging the altimetry data gap and providing water level estimates for regions where the quality and availability of altimetry data are unreliable. In the specific case of our study, Lake Merowe is one such region where the altimetry had very few data points. This study also provides another way of creating a more continuous time series of water levels using a combination of Sentinel and altimetry data, based on their availability. The findings from this study are valuable for water resources management, especially for monitoring reservoir water levels and the corresponding reservoir operations. Such an application of the findings from this study is very critical for transboundary river basins like the Nile, where there are multiple reservoirs in different countries, operated by multiple government bodies. Finally, the availability of improved altimetry data from the SWOT mission will provide an opportunity to build on this study to compare and validate these different approaches in improved water level estimation for inland water bodies.

**Author Contributions:** Conceptualization, P.K. and V.L.; data analysis, P.K.; methodology, P.K., V.L.; validation, P.K.; writing—original draft, P.K.; writing—review and editing, V.L. and P.K. All authors have read and agreed to the published version of the manuscript.

**Funding:** This research received no external funding.

**Data Availability Statement:** Publicly available datasets were analyzed in this study. SRTM data was downloaded from USGS Earth Explorer (<https://earthexplorer.usgs.gov/>, accessed on 15 August 2022). GPM IMERG data was downloaded from NASA Earthdata inventory (<https://search.earthdata.nasa.gov/search>, accessed on 15 August 2022). The Sentinel data was downloaded from the Sentinel hub EO Explorer website (<https://apps.sentinel-hub.com/eo-browser/>, accessed on 15 August 2022).

**Acknowledgments:** The authors acknowledge Benjamin Zaitchik for his contribution in reviewing this manuscript with critical inputs. The first author also acknowledges the support from the Department of Engineering Systems and Environment and from the School of Engineering and Applied Sciences, University of Virginia.

**Conflicts of Interest:** The authors declare no conflict of interest.

## References

1. Alsdorf, D.E.; Rodríguez, E.; Lettenmaier, D.P. Measuring Surface Water from Space. *Rev. Geophys.* **2007**, *45*, 1–24. [[CrossRef](#)]
2. Plengsaeng, B.; Wehn, U.; van der Zaag, P. Data-Sharing Bottlenecks in Transboundary Integrated Water Resources Management: A Case Study of the Mekong River Commission's Procedures for Data Sharing in the Thai Context. *Water Int.* **2014**, *39*, 933–951. [[CrossRef](#)]

3. Gerlak, A.K.; Lautze, J.; Giordano, M. Water Resources Data and Information Exchange in Transboundary Water Treaties. *Int. Environ. Agreem.* **2011**, *11*, 179–199. [[CrossRef](#)]
4. Abd Ellah, R.G. Water Resources in Egypt and Their Challenges, Lake Nasser Case Study. *Egypt. J. Aquat. Res.* **2020**, *46*, 1–12. [[CrossRef](#)]
5. Swain, A. The Nile River Basin Initiative: Too Many Cooks, Too Little Broth. *SAIS Rev.* **2002**, *22*, 293–308. [[CrossRef](#)]
6. Taburet, N.; Zawadzki, L.; Vayre, M.; Blumstein, D.; le Gac, S.; Boy, F.; Raynal, M.; Labroue, S.; Crétaux, J.F.; Femenias, P. S3MPC: Improvement on Inland Water Tracking and Water Level Monitoring from the Oltc Onboard Sentinel-3 Altimeters. *Remote Sens* **2020**, *12*, 3055. [[CrossRef](#)]
7. Ma, Y.; Xu, N.; Sun, J.; Wang, X.H.; Yang, F.; Li, S. Estimating Water Levels and Volumes of Lakes Dated Back to the 1980s Using Landsat Imagery and Photon-Counting Lidar Datasets. *Remote Sens. Environ.* **2019**, *232*, 111287. [[CrossRef](#)]
8. Yuan, C.; Gong, P.; Liu, C.; Ke, C. Water-Volume Variations of Lake Hulun Estimated from Serial Jason Altimeters and Landsat TM/ETM+ Images from 2002 to 2017. *Int. J. Remote Sens.* **2019**, *40*, 670–692. [[CrossRef](#)]
9. Shu, S.; Liu, H.; Beck, R.A.; Frappart, F.; Korhonen, J.; Xu, M.; Yang, B.; Hinkel, K.M.; Huang, Y.; Yu, B. Analysis of Sentinel-3 SAR Altimetry Waveform Retracking Algorithms for Deriving Temporally Consistent Water Levels over Ice-Covered Lakes. *Remote Sens. Environ.* **2020**, *239*, 111643. [[CrossRef](#)]
10. Calmant, S.; Seyler, F.; Cretaux, J.F. Monitoring Continental Surface Waters by Satellite Altimetry. *Surv. Geophys.* **2008**, *29*, 247–269. [[CrossRef](#)]
11. Sharma, K.D.; Singh, S.; Singh, N.; Kalla, A.K. Rôle de La Télédétection Par Satellite Dans La Surveillance Des Ressources En Eau de Surface Dans Un Milieu Aride. *Hydrol. Sci. J.* **1989**, *34*, 531–537. [[CrossRef](#)]
12. Sheffield, J.; Wood, E.F.; Pan, M.; Beck, H.; Coccia, G.; Serrat-Capdevila, A.; Verbist, K. Satellite Remote Sensing for Water Resources Management: Potential for Supporting Sustainable Development in Data-Poor Regions. *Water Resour. Res.* **2018**, *54*, 9724–9758. [[CrossRef](#)]
13. Crétaux, J.F.; Birkett, C. Lake Studies from Satellite Radar Altimetry. *Comptes Rendus Geosci.* **2006**, *338*, 1098–1112. [[CrossRef](#)]
14. Zhang, J.; Xu, K.; Yang, Y.; Qi, L.; Hayashi, S.; Watanabe, M. Measuring Water Storage Fluctuations in Lake Dongting, China, by Topex/Poseidon Satellite Altimetry. *Environ. Monit. Assess.* **2006**, *115*, 23–37. [[CrossRef](#)] [[PubMed](#)]
15. Kansara, P.; Li, W.; El-Askary, H.; Lakshmi, V.; Piechota, T.; Struppa, D.; Sayed, M.A. An Assessment of the Filling Process of the Grand Ethiopian Renaissance Dam and Its Impact on the Downstream Countries. *Remote Sens.* **2021**, *13*, 711. [[CrossRef](#)]
16. Sulistioadi, Y.B.; Tseng, K.H.; Shum, C.K.; Hidayat, H.; Sumaryono, M.; Suhardiman, A.; Setiawan, F.; Sunarso, S. Satellite Radar Altimetry for Monitoring Small Rivers and Lakes in Indonesia. *Hydrol. Earth Syst. Sci.* **2015**, *19*, 341–359. [[CrossRef](#)]
17. Schwatke, C.; Dettmering, D.; Seitz, F. Volume Variations of Small Inland Water Bodies from a Combination of Satellite Altimetry and Optical Imagery. *Remote Sens.* **2020**, *12*, 1606. [[CrossRef](#)]
18. Troitskaya, Y.I.; Rybushkina, G.v.; Soustova, I.A.; Balandina, G.N.; Lebedev, S.A.; Kostyanoi, A.G.; Panyutin, A.A.; Filina, L.v. Satellite Altimetry of Inland Water Bodies. *Water Resour.* **2012**, *39*, 184–199. [[CrossRef](#)]
19. Dettmering, D.; Ellenbeck, L.; Scherer, D.; Schwatke, C.; Niemann, C. Potential and Limitations of Satellite Altimetry Constellations for Monitoring Surface Water Storage Changes—A Case Study in the Mississippi Basin. *Remote Sens.* **2020**, *12*, 3320. [[CrossRef](#)]
20. Li, Y.; Dang, B.; Zhang, Y.; Du, Z. Water Body Classification from High-Resolution Optical Remote Sensing Imagery: Achievements and Perspectives. *ISPRS J. Photogramm. Remote Sens.* **2022**, *187*, 306–327. [[CrossRef](#)]
21. Huang, C.; Chen, Y.; Zhang, S.; Wu, J. Detecting, Extracting, and Monitoring Surface Water From Space Using Optical Sensors: A Review. *Rev. Geophys.* **2018**, *56*, 333–360. [[CrossRef](#)]
22. Bioresita, F.; Puissant, A.; Stumpf, A.; Malet, J.P. A Method for Automatic and Rapid Mapping of Water Surfaces from Sentinel-1 Imagery. *Remote Sens.* **2018**, *10*, 217. [[CrossRef](#)]
23. Schmitt, M. Potential of Large-Scale Inland Water Body Mapping from Sentinel-1/2 Data on the Example of Bavaria’s Lakes and Rivers. *PFG J. Photogramm. Remote Sens. Geoinf. Sci.* **2020**, *88*, 271–289. [[CrossRef](#)]
24. Biancamaria, S.; Lettenmaier, D.P.; Pavelsky, T.M. *The SWOT Mission and Its Capabilities for Land Hydrology*; Springer: Cham, Switzerland, 2016; Volume 37, ISBN 9783319324494.
25. Ebaid, H.M.I.; Ismail, S.S. Lake Nasser Evaporation Reduction Study. *J. Adv. Res.* **2010**, *1*, 315–322. [[CrossRef](#)]
26. Mobasher, A.M.A. Adaptive Reservoir Operation Strategies under Changing Boundary Conditions—The Case of Aswan High Dam Reservoir. Ph.D. Thesis, Darmstadt University of Technology, Darmstadt, Germany, 2010.
27. Kleinitz, C.; Näser, C. The Loss of Innocence: Political and Ethical Dimensions of the Merowe Dam Archaeological Salvage Project at the Fourth Nile Cataract (Sudan). *Conserv. Manag. Archaeol. Sites* **2011**, *13*, 253–280. [[CrossRef](#)]
28. Mulat, A.G.; Moges, S.A.; Moges, M.A. Evaluation of Multi-Storage Hydropower Development in the Upper Blue Nile River (Ethiopia): Regional Perspective. *J. Hydrol. Reg. Stud.* **2018**, *16*, 1–14. [[CrossRef](#)]
29. Alrajoula, M.T.; Al Zayed, I.S.; Elagib, N.A.; Hamdi, M.R. Hydrological, Socio-Economic and Reservoir Alterations of Er Roseires Dam in Sudan. *Sci. Total Environ.* **2016**, *566–567*, 938–948. [[CrossRef](#)]
30. Huffman, G.J.; Bolvin, D.T.; Nelkin, E.J.; Tan, J. IMERG Technical Documentation. Available online: [https://gpm.nasa.gov/sites/default/files/document\\_files/IMERG\\_doc\\_190909.pdf](https://gpm.nasa.gov/sites/default/files/document_files/IMERG_doc_190909.pdf) (accessed on 25 January 2020).
31. Copernicus Sentinel Data Accessed from ESA Open Hub. Available online: <https://scihub.copernicus.eu/dhus/> (accessed on 17 April 2022).

32. Farr, T.G.; Rosen, P.A.; Caro, E.; Crippen, R.; Duren, R.; Hensley, S.; Kobrick, M.; Paller, M.; Rodriguez, E.; Roth, L.; et al. The Shuttle Radar Topography Mission. *Rev. Geophys.* **2007**, *45*, RG2004. [[CrossRef](#)]
33. Tortini, R.; Noujdina, N.; Yeo, S.; Ricko, M.; Birkett, C.M.; Khandelwal, A.; Kumar, V.; Marlier, M.E.; Lettenmaier, D.P. Satellite-Based Remote Sensing Data Set of Global Surface Water Storage Change from 1992 to 2018. *Earth Syst. Sci. Data* **2020**, *12*, 1141–1151. [[CrossRef](#)]
34. Gourgouletis, N.; Bariamis, G.; Anagnostou, M.N.; Baltas, E. Estimating Reservoir Storage Variations by Combining Sentinel-2 and 3 Measurements in the Yliki Reservoir, Greece. *Remote Sens.* **2022**, *14*, 1860. [[CrossRef](#)]
35. Filipponi, F. Sentinel-1 GRD Preprocessing Workflow. *Proceedings* **2019**, *18*, 11.